

201331004A

厚生労働科学研究費補助金

難病・がん等の疾患分野の医療の実用化研究事業（難病関係研究分野）研究事業

神経系疾患の集中的な遺伝子解析及び原因究明に関する拠点研究 に関する研究

平成25年度 総括研究報告書

研究代表者 辻 省次

平成26（2014）年 3月

## 研究報告書目次

### 目 次

I. 総括研究報告 神経系疾患の集中的な遺伝子解析及び原因究明に関する拠点研究 に関する研究 辻 省次	-----	1
II. 研究成果の刊行に関する一覧表	-----	6
III. 研究成果の刊行物・別刷	-----	9

## 研究報告書

厚生労働科学研究費補助金(難病・がん等の疾患分野の医療の実用化研究事業(難病関係研究分野))

### 研究報告書

神経系疾患の集中的な遺伝子解析及び原因究明に関する拠点研究に関する研究

研究代表者 辻 省次・東京大学医学部附属病院神経内科・教授

分担研究者 森下真一・東京大学・新領域創成科学研究科・教授

### 研究要旨

本研究の目的は、次世代シーケンサーを用いた大規模ゲノム配列解析拠点、および、高度のゲノムインフォマティクス拠点を整備し、神経疾患の病因・病態機序を解明することである。次世代シーケンサーを用いた大規模ゲノム解析拠点を整備し、exome 配列解析、全ゲノム配列解析がハイスループットに実施できる体制を構築した。今年度の研究成果として、家族性・孤発性の多系統萎縮症の関連遺伝子を発見した。一般研究拠点、特定疾患調査研究班との協力により、ゲノム解析を進めた。日本人ゲノムの参照配列、variation database の構築を進めた。

#### A. 研究目的

本研究の目的は、次世代シーケンサーを用いた大規模ゲノム配列解析拠点、および、高度のゲノムインフォマティクス拠点を整備し、神経疾患の病因・病態機序を解明することである。また、神経系疾患のゲノム解析拠点として、本研究事業の一般研究や他の難治性疾患研究克服研究事業の研究班などと連携をして、ゲノム解析拠点としての機能を果たし、神経系疾患の病因、病態機序の解明、診断未確定の神経難病の解明などに貢献することを目的としている。本研究の特色は、遺伝性神経疾患、孤発性神経疾患の病因の解明を実現するために、次世代シーケンサーを用いた大規模ゲノム配列解析および高度のゲノムインフォマティクスに基づく研究を強力に推進することにある。

#### B. 研究方法

HiSeq2000 2 台をアップデートして Hiseq2500 に整備した。また、次世代シーケンサーでの解析に必要な robotics の導入など、ゲノム解析のスループットの高いパイプラインを構築し、次世代シーケンサーから産生される膨大なデータを処理するために必要なサーバーシステムを構築した。

研究の方針は、1. 拠点としての技術開発、研究の推進、2. 一般研究拠点との連携に基づく研究、3. 特定疾患調査研究班との連携に基づく研究、4. 日本人ゲノムの variation database の構築、という4つを柱として研究を進めた。

(倫理面への配慮)

ゲノム解析研究は、「ヒトゲノム・遺伝子解析研究に関する倫理指針」に沿って適切に実施

した。研究倫理審査委員会の承認：「神経筋変性疾患の遺伝子解析研究」審査番号 1396-(10) 平成23年8月17日承認

### C. 研究成果

活動方針としては、1. 拠点としての技術開発、研究の推進、2. 一般研究拠点との連携に基づく研究、3. 特定疾患長鎖研究班との連携に基づく研究、4. 日本人ゲノムの variation database の構築、を柱として研究を進めた。

**拠点としての技術開発、研究の推進：**遺伝性神経疾患の病因遺伝子の解明、孤発性神経疾患の疾患発症に関連する遺伝子の解明をめざした。遺伝性神経疾患については、家族性筋萎縮性側索硬化症、家族性認知症疾患、家族性てんかん、家族性ミオパチーをはじめとして、研究を進めており、これまでにわれわれが開発したハイスループットの連鎖解析システム (SNP HiTLink) を用いた解析と、exome/全ゲノム解析を統合的に進めた。今年度は、家族性・孤発性の多系統萎縮症の関連遺伝子 *COQ2* を同定した (Mitsui et al. New Engl. J. Med. 2013)。また、家族性筋萎縮性側索硬化症の病因遺伝子を発見した (Takahashi et al. Amer. J. Hum. Genet. 2013)。以上のように、遺伝性神経疾患だけでなく、孤発性神経疾患を対象として、次世代シーケンサーを駆使したゲノム解析は順調な成果を上げている。

遺伝子診断への応用としては、若年発症の脊髄小脳変性症に対して、次世代シーケンサーを用いた網羅的な解析を行い、病因遺伝子の一つである *SETX* の病原性変異を同定し、報告した (Ichikawa et al. J. Neurol. Sci. 2013)。

**一般研究拠点との連携に基づく研究：**遺伝性末梢神経疾患 (Charcot-Marie-Tooth 病)、ミオパチー、HTLV-1 関連脊髄症など 591 例について全エクソーム配列解析を完了した。進行性核上性麻痺についても、検体収集体制の構築が行われ、現在までに、51 件の全エクソーム配列

解析を完了した。これらのデータに基づく研究が一般研究拠点の方で順調に進んでいる。孤発例に対して、exome 解析による関連解析を実施する上では、コントロールの規模の大きさが検出力に大きく影響することから、大規模コントロールの variation database は、本研究班のみならず、わが国のゲノム医学研究においても必須の研究リソースとなると考えられる。そこで、神経系の一般研究拠点と連携して、コントロールの variation database の整備を進めており、全拠点で、新たに IRB 承認を得た上で、1,000 名規模の日本人ゲノムの variation database を整備し、公開する予定である。

**特定疾患調査研究班との連携に基づく研究：**これまでに神経変性班、運動失調班などとの連携が進んでおり、あわせて、exome 81 例、全ゲノム解析 1 例の実績があり、各研究機関の研究を支援する機能を果たしている。

**日本人ゲノムの variation database の構築：**exome 解析に基づく関連解析では、コントロールのサンプルサイズが検出力に大きく影響することから、日本人ゲノムの variation database の整備を進めている。さらに、5 拠点で協力して、1,208 名規模の日本人ゲノムの variation database を整備し、公開した

(<http://www.genome.med.kyoto-u.ac.jp/SnpDB/>)。

### D. 考察

次世代シーケンサーの解析システムの整備として、Illumina 社の HiSeq2500 を 2 台導入したこと、さらに、サンプル調製のために robotics を導入したことにより、ゲノム解析のスループットが著しく強化されたこと、また、そこから産生される膨大な規模のデータを処理するための、計算サーバーシステムを整備したことにより、大規模サンプルのゲノム配列解析が、それほど大きな負担なく実施できるようになったことが、なによりも大きな成果である。

このことにより、われわれの研究プロジェクトの遂行はもちろんのこと、一般研究拠点や、他の特定疾患調査研究班からの依頼を引き受けることができるようになったことが大きな成果として評価できる。

研究成果としては、家族性・孤発性の多系統萎縮症の関連遺伝子として *COQ2*、家族性筋萎縮性側索硬化症の病因遺伝子として *ERBB4* を発見したことは大きな成果である。多系統萎縮症、筋萎縮性側索硬化症はともに有効な治療法のない神経変性疾患であるが、発見された病因遺伝子は機能的によく知られている遺伝子であり、治療法開発の手掛かりの一つになると期待される。

難病の遺伝子診断への応用という点では、若年発症の脊髄小脳変性症の遺伝子診断への応用 (Ichikawa et al. *J. Neurol. Sci.* 2013) も評価できる研究成果であると言える。

次世代シーケンサーを遺伝子診断に応用するという点では、それぞれの疾患において、解析候補となる遺伝子型数となる場合が多く、次世代シーケンサーの役割が非常に大きくなってきている。一方、医療の中に定着させていくためには、保険収載、あるいは、先進医療などの実現を検討する必要がある。従来は、わが国においては、研究の一環としての遺伝子解析を診療に応用することが多かったが、研究における遺伝子解析と、診療への遺伝子解析の提供を区別していくことが重要になってきている。後者は、わが国の医療の体制の中では、保険収載、あるいは、先進医療としての実現が求められるところであるが、体外診断法については、薬事法に基づく薬事承認が前提条件となるが、このような先進的な技術を用いた体外診断法を、薬事承認するということは、前例のないことであり、検討すべき課題が多い。

最近のゲノム研究の成果から、農耕文明の定着に伴った人口爆発により、それぞれの人種において、ethnicity-specific な variation が多数

集積されていることが示されている。このようなことから、日本人のゲノム解析研究においては、日本人ゲノムの参照配列や variation の頻度情報を用いることが重要である。逆に、これまでもわが国の研究のように、欧米人ゲノム情報を参照配列とした場合は、ノイズが非常に大きくなり、研究の遂行に支障を来しやすいことが明らかになってきている。このような背景から、1,208人の日本人健康者について、日本人ゲノムの多様性に関する頻度情報を公開した。このようなデータは、わが国の研究者コミュニティが積極的にそれぞれの研究に活用でき、その意義は大きいと考え、この点でも、本研究拠点（5拠点）の成果として重要である。

## E. 結論

次世代シーケンサーを用いた解析拠点の構築を行い、遺伝性神経疾患、孤発性神経疾患の発症に関わる新規の遺伝子を2つ見出した。また、数多くの診断未確定の疾患に対して診断を確定することができた。一般研究、難治性疾患克服研究事業の研究班と積極的に連携し、次世代シーケンサーを用いた解析を行い、拠点としての役割を果たした。

## F. 健康危険情報

該当事項なし。

## G. 研究発表

### 1. 論文発表

1. Ishii A, Saito Y, Mitsui J, Ishiura H, Yoshimura J, Arai H, Yamashita S, Kimura S, Oguni H, Morishita S, Tsuji S, Sasaki M, Hirose S. Identification of ATP1A3 mutations by exome sequencing as the cause of alternating hemiplegia of childhood in Japanese patients. *PLOS One* 8:e56120, 2013
2. Miyashita A, Koike A, Jun G, Wang L-S,

- Takahashi S, Matsubara E, Kawarabayashi T, Shoji M, Tomita N, Arai H, Asada T, Harigaya Y, Ikeda M, Amari M, Hanyu H, Higuchi S, Ikeuchi T, Nishizawa M, Suga M, Kawase Y, Akatsu H, Kosaka K, Yamamoto T, Imagawa M, Hamaguchi T, Yamada M, Moriaha T, Takeda M, Takao T, Nakata K, Fujisawa Y, Sasaki K, Watanabe K, Nakashima K, Urakami K, Ooya T, Takahashi M, Yuzuriha T, Serikawa T, Yoshimoto S, Nakagawa R, Kim J-W, Ki C-S, Won H-H, Na DL, Seo SW, Mook-Jung I, The Alzheimer Disease Genetics Consortium, St. George-Hyslop P, Mayeux R, Haines JL, Pericak-Vance MA, Yoshida M, Nishida N, Tokunaga K, Yamamoto K, Tsuji S, Kanazawa I, Ihara Y, Schellenberg GD, Farrer LA. and Kuwano R. SORL1 Is Genetically Associated with Late-Onset Alzheimer's Disease in Japanese, Koreans and Caucasians. *PLoS ONE* 8: e58618, 2013
3. Ichikawa Y, Ishiura H, Mitsui J, Takahashi Y, Kobayashi S, Takuma H, Kanazawa I, Doi K, Yoshimura J, Morishita S, Goto J, Tsuji S. Exome analysis reveals a Japanese family with spinocerebellar ataxia, autosomal recessive 1. *J. Neurol. Sci.*;331:158-60, 2013.
  4. Mitsui J, Matsukawa T, Ishiura H, Fukuda Y, Ichikawa Y, Date H, Ahsan B, Nakahara Y, Momose Y, Takahashi Y, Iwata A, Goto J, Yamamoto Y, Komata M, Shirahige K, Hara K, Kakita A, Yamada M, Takahashi H, Onodera O, Nishizawa M, Takashima H, Kuwano R, Watanabe H, Ito M, Sobue G, Soma H, Yabe I, Sasaki H, Aoki M, Ishikawa K, Mizusawa H, Kanai K, Hattori T, Kuwabara S, Arai K, Koyano S, Kuroiwa Y, Hasegawa K, Yuasa T, Yasui K, Nakashima K, Ito H, Izumi Y, Kaji R, Kato T, Kusunoki S, Osaki Y, Horiuchi M, Kondo T, Murayama S, Hattori N, Yamamoto M, Murata M, Satake W, Toda T, Dürr A, Brice A, Filla A, Klockgether T, Wüllner U, Nicholson G, Gilman S, Shults CW, Tanner CM, Kukull WA, Lee V M-Y, Masliah E, Low PA, Sandroni P, Trojanowski JQ, Ozelius L, Foroud T, and Tsuji S. Mutations of COQ2 in familial and sporadic multiple system atrophy. *New Engl. J. Med.* 369:233-44, 2013
  5. Landouré G, Zhu PP, Lourenço CM, Johnson JO, Toro C, Bricceno KV, Rinaldi C, Meilleur KG, Sangaré M, Diallo O, Pierson TM, Ishiura H, Tsuji S, Hein N, Fink JK, Stoll M, Nicholson G, Gonzalez MA, Speziani F, Dürr A, Stevanin G, Biesecker LG; NIH Intramural Sequencing Center, Accardi J, Landis DM, Gahl WA, Traynor BJ, Marques W Jr, Züchner S, Blackstone C, Fischbeck KH, Burnett BG. Hereditary spastic paraplegia type 43 (SPG43) is caused by mutation in C19ORF12. *Human Mutation* 34:1357-60, 2013
  6. Isojima T, Doi K, Mitsui J, Oda Y, Tokuhiro E, Yasoda A, Yorifuji T, Horikawa R, Yoshimura J, Ishiura H, Morishita S, Tsuji S, and Kitanaka S. A recurrent de novo FAM111A mutation causes Kenny–Caffey syndrome type 2. *J Bone Mineral Res.* 29: 992-998, 2013
  7. Sasaki M, Ishii A, Saito Y, Morisada N,

Iijima K, Takada S, Araki A, Tanabe Y, Arai H, Yamashita S, Ohashi T, Oda Y, Ichiseki H, Hirabayashi S, Yasuhara A, Kawawaki H, Kimura S, Shimono M, Narumiya M, Suzuki M, Yoshida T, Oyazato Y, Tsuneishi S, Ozasa S, Yokochi K, Dejima S, Akiyama T, Kishi N, Kira R, Ikeda T, Oguni H, Zhang B, Tsuji S and Hirose S. Genotype–Phenotype Correlations in Alternating Hemiplegia of Childhood Neurology 82: 482-90, 2014

8. Yamada M, Tanaka M, Takagi M, Kobayashi S, Taguchi Y, Takashima S, Tanaka K, Touge T, Hatsuta H, Murayama S, Hayashi Y, Kaneko M, Ishiura H, Mitsui J, Astuta N, Sobue G, Shimozawa N, Inuzuka T, Tsuji S, and Hozumi I. Evaluation of SLC20A2 mutations that cause idiopathic basal ganglia calcification in Japan. *Neurol.* 82: 705-712, 2014
9. Ishiura H, Takahashi Y, Hayashi T, Saito K, Furuya H, Watanabe M, Murata M, Suzuki M, Sugiura A, Sawai S, Shibuya K, Ueda N, Ichikawa Y, Kanazawa I, Goto J, Tsuji S. Molecular epidemiology and clinical spectrum of hereditary spastic paraplegia in the Japanese population based on comprehensive mutational analyses. *J. Hum. Genet.* 59: 163-72, 2014

#### H. 知的財産権の出願・登録状況

(予定を含む。)

##### 1 特許取得

多系統萎縮症リスクの検査方法, 検査キット, 及び多系統萎縮症の治療又は予防薬 (特願 2013-20763)

#### 2. 実用新案登録

該当無し

研究成果の刊行に関する一覧表

雑誌

発表者氏名	論文タイトル名	発表誌名	巻号	ページ	出版年
Ishii A, Saito Y, Mitsui J, Ishiura H, Yoshimura J, Ara i H, Yamashita S, Kimura S, Oguni H, Morishita S, Tsuji S, Sasaki M, Hirose S.	Identification of A TP1A3 mutations by exome sequencing as the cause of alternating hemiplegia of childhood in Japanese patients.	<i>PLOS One</i>	8	E56120	2013
Miyashita A, Koike A, Jun G, Wang L-S, Takahashi S, Matsubara E, Kawarabayashi T, Shoji M, Tomita N, Arai H, Asada T, Harigaya Y, Ikeda M, Amari M, Hanyu H, Higuchi S, Ikeuchi T, Nishizawa M, Suga M, Kawas e Y, Akatsu H, Kosaka K, Yamamoto T, Imagawa M, Hamaguchi T, Yamada M, Moriaha T, Takeda M, Taka o T, Nakata K, Fujisawa Y, Sasaki K, Watanabe K, Nakashima K, Urakami K, Ooya T, Takahashi M, Yuzuriha T, Serikawa T, Yoshimoto S, Nakagawa R, Kim J-W, Ki C-S, Won H-H, Na DL, Seo SW, Mook-Jung I, The Alzheimer Disease Genetics Consortium, St. George-Hyslop P, Mayeux R, Haines JL, Pericak-Vance MA, Yoshida M, Nishida N, Tokunaga K, Yamamoto K, Tsuji S, Kanazawa I, Ihara Y, Schellenberg GD, Farrer LA. and Kuro wano R.	SORL1 Is Genetically Associated with Late-Onset Alzheimer's Disease in Japanese, Koreans and Caucasians.	<i>PLoS ONE</i>	8	E58618	2013
Ichikawa Y, Ishiura H, Mitsui J, Takahashi Y, Kobayashi S, Takuma H, Kanazawa I, Doi K, Yoshimura J, Morishita S, Goto J, Tsuji S.	Exome analysis reveals a Japanese family with spinocerebellar ataxia, autosomal recessive 1.	<i>J. Neurol. Sci.</i>	331	158-60	2013



<p>Mitsui J, Matsukawa T, Ishiura H, Fukuda Y, Ichikawa Y, Date H, Ahsan B, Nakahara Y, Momose Y, Takahashi Y, Iwata A, Go to J, Yamamoto Y, Komata M, Shirahige K, Hara K, Kakita A, Yamada M, Takahashi H, Onodera O, Nishizawa M, Takashima H, Kuwano R, Watanabe H, Ito M, Sobue G, Soma H, Yabe I, Sasaki H, Aoki M, Ishikawa K, Mizusawa H, Kanai K, Hattori T, Kuwabara S, Arai K, Koyano S, Kuroiwa Y, Hasegawa K, Yuasa T, Yasui K, Nakashima K, Ito H, Izumi Y, Kaji R, Kato T, Kusunoki S, Osaki Y, Horiuchi M, Kondo T, Murayama S, Hattori N, Yamamoto M, Murata M, Satake W, Toda T, Dürr A, Brice A, Filla A, Klockgether T, Willner U, Nicholson G, Gilman S, Shults CW, Tanner CM, Kukull WA, Lee V M-Y, Masliah E, Low PA, Sandroni P, Trojanowski JQ, Ozelius L, Foroud T, and Tsuji S.</p>	<p>Mutations of COQ2 in familial and sporadic multiple system atrophy.</p>	<p><i>New Engl. J. Med.</i></p>	<p>369</p>	<p>233-44</p>	<p>2013</p>
<p>Landouré G, Zhu PP, Lourenço CM, Johnson JO, Toro C, Bricceno KV, Rinaldi C, Meilleur KG, Sangaré M, Diallo O, Pierson TM, Ishiura H, Tsuji S, Hein N, Fink JK, Stoll M, Nicholson G, Gonzalez MA, Speziani F, Dürr A, Stevanin G, Biesecker LG; NIH Intramural Sequencing Center, Accardi J, Landis DM, Gahl WA, Traynor BJ, Marques W Jr, Züchner S, Blackstone C, Fischbeck KH, Burnett BG.</p>	<p>Hereditary spastic paraplegia type 43 (SPG43) is caused by mutation in C19ORF12.</p>	<p><i>Human Mutation</i></p>	<p>34</p>	<p>1357-60</p>	<p>2013</p>
<p>Isojima T, Doi K, Mitsui J, Oda Y, Tokuhiko E, Yasoda A, Yorifuji T, Horikawa R, Yoshimura J, Ishiura H, Morishita S, Tsuji S, and Kitanaka S.</p>	<p>A recurrent de novo FAM111A mutation causes Kenny-Caffey syndrome type 2.</p>	<p><i>J Bone Mineral Res.</i></p>	<p>29</p>	<p>992-8</p>	<p>2013</p>

Sasaki M, Ishii A, Saito Y, Morisada N, Iijima K, Takada S, Araki A, Tanabe Y, Arai H, Yamashita S, Ohashi T, Oda Y, Ichiseki H, Hirabayashi S, Yasuhara A, Kawawaki H, Kimura S, Shimono M, Narumiya M, Suzuki M, Yoshida T, Oyazato Y, Tsuneishi S, Ozasa S, Yokochi K, Dejima S, Akiyama T, Kishi N, Kira R, Ikeda T, Oguni H, Zhang B, Tsuji S and Hirose S.	Genotype–Phenotype Correlations in Alternating Hemiplegia of Childhood	<i>Neurology</i>	82	482-90	2014
Yamada M, Tanaka M, Takagi M, Kobayashi S, Taguchi Y, Takashima S, Tanaka K, Touge T, Hatsuta H, Murayama S, Hayashi Y, Kaneko M, Ishiura H, Mitsui J, Astuta N, Sobue G, Shimozawa N, Inuzuka T, Tsuji S, and Hozumi I.	Evaluation of SLC20A2 mutations that cause idiopathic basal ganglia calcification in Japan.	<i>Neurology</i>	82	705-12	2014
Ishiura H, Takahashi Y, Hayashi T, Saito K, Furuya H, Watanabe M, Murata M, Suzuki M, Sugiura A, Sawai S, Shibuya K, Ueda N, Ichikawa Y, Kanazawa I, Goto J, Tsuji S.	Molecular epidemiology and clinical spectrum of hereditary spastic paraplegia in the Japanese population based on comprehensive mutational analyses.	<i>J. Hum. Genet.</i>	59	163-72	2014

## Hereditary Spastic Paraplegia Type 43 (SPG43) is Caused by Mutation in *C19orf12*

Guida Landouré,<sup>1,2\*</sup> Peng-Peng Zhu,<sup>2</sup> Charles M. Lourenço,<sup>3</sup> Janel O. Johnson,<sup>4</sup> Camilo Toro,<sup>5</sup> Katherine V. Bricceno,<sup>2</sup> Carlo Rinaldi,<sup>2</sup> Katherine G. Meilleur,<sup>6</sup> Modibo Sangaré,<sup>2</sup> Oumarou Diallo,<sup>2</sup> Tyler M. Pierson,<sup>2,5</sup> Hiroyuki Ishiura,<sup>7</sup> Shoji Tsuji,<sup>7</sup> Nichole Hein,<sup>8</sup> John K. Fink,<sup>8,9</sup> Marion Stoll,<sup>10</sup> Garth Nicholson,<sup>10</sup> Michael A. Gonzalez,<sup>11</sup> Fiorella Speziani,<sup>11</sup> Alexandra Dürr,<sup>12,13</sup> Giovanni Stevanin,<sup>12,13,14</sup> Leslie G. Biesecker,<sup>15</sup> for the NIH Intramural Sequencing Center, John Accardi,<sup>5</sup> Dennis M. D. Landis,<sup>5</sup> William A. Gahl,<sup>5</sup> Bryan J. Traynor,<sup>4</sup> Wilson Marques Jr,<sup>3</sup> Stephan Züchner,<sup>11</sup> Craig Blackstone,<sup>2</sup> Kenneth H. Fischbeck,<sup>2</sup> and Barrington G. Burnett<sup>2</sup>

<sup>1</sup>Service de Neurologie, Centre Hospitalier Universitaire du Point "G", Bamako, Mali; <sup>2</sup>Neurogenetics Branch, National Institute of Neurological Disorders and Stroke, National Institutes of Health, Bethesda, Maryland; <sup>3</sup>Department of Neuroscience and Behaviour Sciences, School of Medicine of Ribeirão Preto, University of Sao Paulo, Sao Paulo, Brazil; <sup>4</sup>Laboratory of Neurogenetics, National Institute on Aging, National Institutes of Health, Bethesda, Maryland; <sup>5</sup>NIH Undiagnosed Diseases Program, NIH Common Fund, Office of the Director, National Institutes of Health, Bethesda, Maryland; <sup>6</sup>Tissue Injury Branch, National Institute of Nursing Research, National Institutes of Health, Bethesda, Maryland; <sup>7</sup>Department of Neurology, Graduate School of Medicine, University of Tokyo, Tokyo, Japan; <sup>8</sup>Department of Neurology, University of Michigan Medical School, Ann Arbor, Michigan; <sup>9</sup>Geriatric Research Education and Clinical Center, Ann Arbor Veterans Affairs Medical Center, University of Michigan, Ann Arbor, Michigan; <sup>10</sup>Northcott Neuroscience Laboratory, ANZAC Research Institute, University of Sydney, Sydney, Australia; <sup>11</sup>Department of Human Genetics and John P. Hussman Institute for Human Genomics, University of Miami Miller School of Medicine, Miami, Florida; <sup>12</sup>AP-HP, Department of Genetics and Cytogenetics, Pitié-Salpêtrière Hospital, Paris, France; <sup>13</sup>Centre de Recherche de l'Institut du Cerveau et de la Moelle épinière, INSERM/UPMC UMRS975, CNRS UMR7225, Pitié-Salpêtrière Hospital, Paris, France; <sup>14</sup>Ecole Pratique des Hautes Etudes (EPHE), Paris, France; <sup>15</sup>Genetic Disease Research Branch and NIH Intramural Sequencing Center, National Institutes of Health, Bethesda, Maryland

Communicated by Lars Bertram

Received 21 December 2012; accepted revised manuscript 30 June 2013.

Published online 15 July 2013 in Wiley Online Library (www.wiley.com/humanmutation). DOI: 10.1002/humu.22378

**ABSTRACT:** We report here the genetic basis for a form of progressive hereditary spastic paraplegia (SPG43) previously described in two Malian sisters. Exome sequencing revealed a homozygous missense variant (c.187G>C; p.Ala63Pro) in *C19orf12*, a gene recently implicated in neurodegeneration with brain iron accumulation (NBIA). The same mutation was subsequently also found in a Brazilian family with features of NBIA, and we identified another NBIA patient with a three-nucleotide deletion (c.197\_199del; p.Gly66del). Haplotype analysis revealed that the p.Ala63Pro mutations have a common origin, but MRI scans showed no brain iron deposition in the Malian SPG43 subjects. Heterologous expression of these SPG43 and NBIA variants resulted in similar alterations in the subcellular distribution of *C19orf12*. The SPG43 and NBIA variants reported here as well as the most common *C19orf12* missense mutation reported in NBIA patients are found within a highly conserved,

extended hydrophobic domain in *C19orf12*, underscoring the functional importance of this domain.

Hum Mutat 34:1357–1360, 2013. Published 2013 Wiley Periodicals, Inc.\*\*

**KEY WORDS:** SPG43; NBIA; *C19orf12*; hereditary spastic paraplegia

Hereditary spastic paraplegias (HSPs) are heterogeneous neurological disorders (SPG1–57) characterized by progressive spasticity and weakness in the lower limbs [Harding, 1993]. The estimated prevalence is about 3–9/100,000 in most populations [Blackstone et al., 2011; Erichsen et al., 2009; Silva et al., 1997]. All modes of inheritance have been described, but dominant HSPs are most common in North America and northern Europe, whereas recessive forms are predominant in North Africa, the Middle East, and the Mediterranean region [Erichsen et al., 2009; Harding, 1993; Silva et al., 1997]. Over 30 recessive HSPs have been described, and over 20 of the disease genes have been identified to date.

In HSPs, axons of the corticospinal tracts and posterior columns of the spinal cord are impaired in a length-dependent manner. The cellular pathophysiology of HSPs involves several functional areas, including organellar membrane shaping and traffic, mitochondrial function, myelination, and lipid and cholesterol metabolism [Blackstone et al., 2011; Blackstone, 2012]. Some HSP proteins have been implicated in more than one of these areas. For example, SPG4, the most common form of HSP, is caused by mutations in *SPAST* (MIM #604277), the gene encoding spastin, an ATPase involved in endoplasmic reticulum (ER) morphogenesis, endosomal

Additional Supporting Information may be found in the online version of this article.

\*Correspondence to: Guida Landouré, Service de Neurologie, Centre Hospitalier Universitaire du Point "G", Point "G", Bamako, PO Box: 333, Mali. E-mail: landoureg@ninds.nih.gov

Contract grant sponsors: NIH/NINDS Intramural Research Funds (1ZIA NS002974-13); NHGRI; NIH (R01NS072248, R01NS054132); l'Agence Nationale pour la Recherche (SPAX); VERUM Foundation and Association Strümpell-Lorrain.



trafficking, BMP signaling, cytokinesis, and cytoskeletal regulation [Hazan et al., 1999].

We previously described a consanguineous Malian family with recessive HSP in which two sisters presented at the age of 7 and 12 years with gait difficulty, spasticity, and peripheral neuropathy, and shared a region of extended homozygosity on chromosome 19 [Meilleur et al., 2010]. Five years after the initial examination, the older patient had severe atrophy and decreased sensation in the arms and legs, and reduced-to-absent reflexes, but no cognitive decline, facial and bulbar weakness, or vision loss. Brain MRI of one of the affected sisters showed no abnormalities, in particular no brain iron deposits (Fig. 1A). DNA from an affected sister was used to perform exome sequencing as previously described [Landouré et al., 2012], and we identified a homozygous missense sequence variant in the coding region of the *C19orf12* gene (NM\_001031726.3; MIM #614297) at position c.187G>C (Supp. Fig. S1), predicting the amino-acid substitution p.Ala63Pro (http://databases.lovd.nl/shared/variants/C19orf12). Sequencing of 298 Malian controls did not show the homozygous sequence variant. The sequence variant was also not seen in 951 samples in the ClinSeq® cohort [Biesecker et al., 2009]. Interestingly, the variant was found in three of 3,836 African-American alleles (but none of 8,222 European-American alleles) in the NHLBI Exome Sequencing Project database (http://evs.gs.washington.edu/EVS/). We subsequently sequenced the full coding region of *C19orf12* in 16 Australians, 46 French, 195 Americans, and 170 Japanese presenting with diverse HSP types, and none had the c.187G>C variant or any other detectable variant in the gene. Thus, *C19orf12* mutation is likely a rare cause of autosomal recessive HSP.

While this work was in progress, mutations in *C19orf12* were reported in a series of patients with neurodegeneration with brain iron accumulation (NBIA) [Hartig et al., 2011]. NBIA is a heterogeneous neurological disorder caused by mutations in a range of genes, some of which display allelic heterogeneity [Paisan-Ruiz et al., 2009]. It is characterized primarily by extrapyramidal features, with spasticity and optic atrophy. Psychiatric symptoms and cognitive decline have been reported in some cases [Hartig et al., 2011]. We evaluated an NBIA patient at the NIH Clinical Center under the auspices of the NIH Undiagnosed Diseases Program. The subject presented at the age of 4 years with speech difficulty followed by progressive spasticity and impaired walking. On examination, he had dysarthria, psychomotor slowness, brisk reflexes, mild weakness and atrophy in the distal extremities, and small, pale optic discs. Electromyography showed denervation changes over multiple body segments, worse distally, consistent with a motor neuropathy. Brain MRI imaging showed symmetrical excess iron deposition in the globus pallidus (Fig. 1B). Exome sequencing identified a previously reported in-frame deletion in the coding region of the *C19orf12* gene (c.197\_199del, p.Gly66del) [Deschauer et al., 2012].

We also evaluated a consanguineous Brazilian family in which two affected siblings presented with walking difficulties at the age of 14 and 15 years. Their clinical examinations showed spasticity, distal wasting, weakness, reduced sensation, and visual loss with bilateral optic atrophy. They became wheelchair-bound in their mid-thirties. Electrodiagnostic studies showed an axonal sensory and motor neuropathy, and MRI scans showed evidence of brain iron deposits in the globus pallidus (Supp. Fig. S2). The younger sibling had memory loss and depression, but the older sibling had no psychiatric features. Using the GEM.app software [Gonzalez et al., 2013] to analyze exome sequencing data, we identified the same variant seen in the Malian family (Ala63>Pro). An analysis of the markers around the *C19orf12* locus showed that the Malian and Brazilian families had a shared haplotype, indicating that the variants likely have a

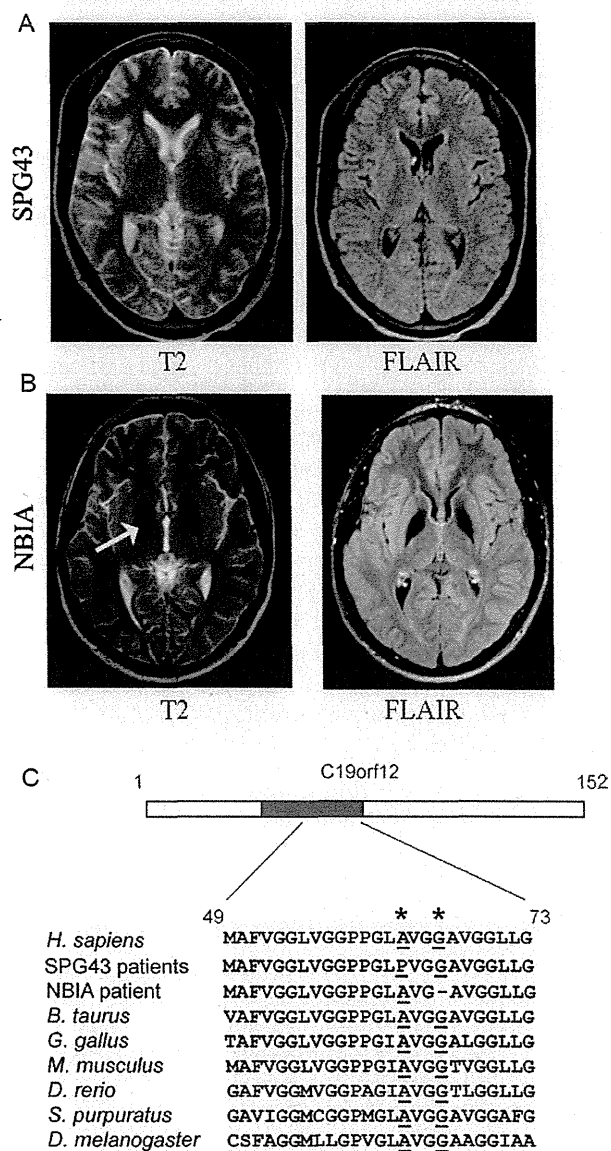


**Figure 1.** MRI and genetic characterization of SPG43 and NBIA. **A:** Brain MRI images of a SPG43 subject with the homozygous *C19orf12* mutation c.187G>C, p.Ala63Pro. **B:** MRI images of a NBIA patient with the homozygous *C19orf12* deletion c.197\_199GG, p.Gly66del. The white arrow indicates iron deposition. **C:** Schematic diagram of *C19orf12*, with the hydrophobic sequence in blue, and a protein sequence alignment of *C19orf12* in various species (amino acid numbers refer to the human sequence). The SPG43 and NBIA mutations cause amino acid changes at Ala63 and Gly66, respectively, both highly conserved residues (in red, asterisks above).

common origin (Supp. Table S1). The Ala63 and Gly66 residues are conserved across a wide range of species including mammals, fish, and insects, indicating functional importance (Fig. 1C).

Computational analyses (http://www.predictprotein.org/) predict that the Ala63 and Gly66 residues are within a membrane domain. The extended nature of this hydrophobic domain and the presence of single or paired Pro residues within the region in all known species further raises the possibility that this domain forms a hydrophobic hairpin, as has been described in many ER proteins mutated in other HSPs, including the three most common forms

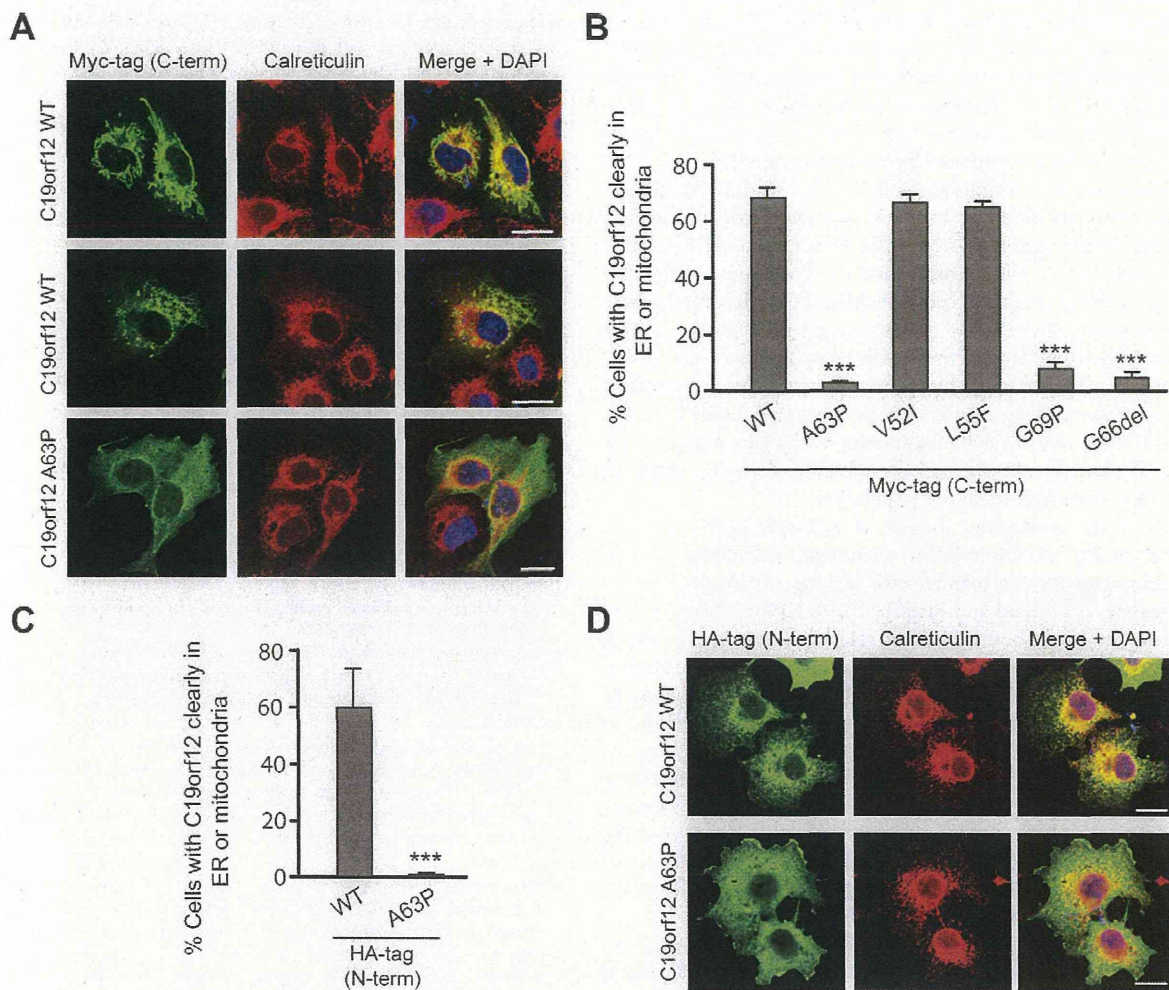


**Figure 2.** *C19orf12* localizes to the ER, and the SPG43 and NBIA mutations alter its subcellular distribution. **A:** COS7 cells expressing HA-tagged wild-type (WT) or p.Ala63Pro mutant *C19orf12* were costained for endogenous calreticulin, an ER protein (red). **B:** Quantification of the subcellular distribution of *C19orf12* in cells expressing Myc-tagged, wild-type *C19orf12* or *C19orf12* containing the SPG43 mutation p.Ala63Pro, the NBIA-associated mutants p.Gly69Arg and p.Gly66del, or two known polymorphisms (p.Val52Ile and p.Leu55Phe). Cells with *C19orf12* clearly at the ER or mitochondria were counted ( $n = 3$  trials, with >100 cells per trial). **C** and **D:** Cells expressing HA-tagged wild-type or p.Ala63Pro mutant *C19orf12* (green) were coimmunostained for calreticulin (red) and DAPI (blue) (**D**) and their distributions quantitated (**C**) as in panel B. Data represent the means  $\pm$  SEM of three independent, blinded experiments. C-term, C-terminal; N-term, N-terminal. \*\*\*  $P < 0.001$ . Bars, 20  $\mu$ m.

[Blackstone, 2012]. In any case, the p.Ala63Pro mutation is very likely to be disruptive. We found that, in cultured cells, recombinant N-terminally tagged wild-type *C19orf12* had a complex and variable distribution. In many cells, it colocalized closely with the ER marker calreticulin, whereas in some other cells, *C19orf12* appeared to localize more to mitochondria (Fig. 2A and Supp. Fig. S3A). The p.Ala63Pro missense mutant showed a dramatically different, more generalized distribution throughout the cytoplasm in a majority of cells, similar to p.Gly66del and another commonly reported NBIA mutant (p.Gly69Arg) [Hartig et al., 2011] (Fig. 2A and B and Supp. Fig. S3B). However, known polymorphisms in healthy controls, p.Val52Ile and p.Leu55Phe, which are also in the predicted membrane domain, did not alter the subcellular localization (Fig. 2B). The position of the epitope tag did not appear to influence these findings, since expression of an N-terminally HA-tagged *C19orf12* protein gave results similar to those of C-terminal Myc-

tagged *C19orf12* for both the wild-type and p.Ala63Pro mutant proteins (Fig. 2C and D).

A previous NBIA study localized *C19orf12* to mitochondria [Hartig et al., 2011]. Our studies of recombinant wild-type *C19orf12* show a complex localization to a variety of organelles, primarily the ER but also the mitochondria (Fig. 2 and Supp. Fig. S2A). In future studies, it will be important to investigate the localization of the endogenous *C19orf12* protein in more detail, with a particular focus on ER, mitochondria, and ER–mitochondrial contact sites.

SPG43 is an autosomal recessive spastic paraplegia with a presentation that includes distal amyotrophy, whereas NBIA is characterized by extrapyramidal and psychiatric features, optic atrophy, cognitive decline, and brain iron deposits in addition to spasticity. In this study, we show that *C19orf12* mutation can present with or without typical features of NBIA, that is, that it can cause spastic paraplegia with lower motor neuron features (SPG43) without



vision loss and brain iron accumulation, as in the Malian family, or with vision loss and evidence of brain iron accumulation but without extrapyramidal features (dystonia and parkinsonism), as in the Brazilian family. These findings are an important extension of the phenotype previously reported with *C19orf12* mutation [Hogarth et al., 2013] to include HSP and formes frustes of NBIA.

The differences in phenotype could be due to different genetic or environmental modifiers in the Malian and Brazilian families. With the shared haplotype around the locus, the p.Ala63Pro mutation likely has a common origin and other variations within the gene are unlikely, but there could be different modifiers elsewhere in the genome. Alternatively the phenotypic differences could be stochastic. It is unlikely that they are due to a difference in the evaluations, since both families had thorough neurological exams and MRI brain scans. The presence of the heterozygous p.Ala63Pro mutation in about one in 1,300 African-American alleles indicates that it may be a rare, previously unidentified cause of spastic paraplegia or NBIA in homozygotes in this population.

One of the pathogenic themes of recessive HSP mutations is abnormality of intracellular membrane trafficking, a process important for the maintenance of long corticospinal axons [Blackstone, 2012; Reid and Rugarli, 2010]. *C19orf12* is predicted to be a membrane-bound protein [Hartig et al., 2011], with a long hydrophobic domain extending from approximately amino-acid residues 42–75. As with the mutations described in this study, mutations in most patients with NBIA cluster within the predicted helical membrane domain, highlighting its potentially important functional role. The mutations identified here and the p.Gly69Arg mutation described in other patients with NBIA, but not known polymorphisms in the predicted membrane domain, disrupt the subcellular distribution of *C19orf12*, indicating that the altered localization of the disease-causing mutations may contribute to the pathologic mechanism.

Although the cellular functions of *C19orf12* remain unclear, an interesting parallel is seen with the clinical spectrum of *FA2H* (MIM #611026) mutations. This gene is mutated in SPG35 as well as NBIA and leukodystrophy [Kruer et al., 2010]. The *FA2H* gene product functions in fatty acid synthesis; the *C19orf12* mutation characterized here alters subcellular localization of *C19orf12* to the ER and may affect similar pathways. Furthermore, the phospholipase A2 gene *PLA2G6* (MIM #603604) is mutated in autosomal recessive NBIA, and this enzyme is involved in the metabolism of complex lipids [Lamari et al., 2013]. Although patients with NBIA present with features not seen in the SPG43 siblings, some overlapping findings are present, indicating that mutations in *C19orf12* can also present across a neurological disease spectrum. Further functional and localization studies of *C19orf12* should shed light on any common cellular mechanisms by which the mutations result in common clinical manifestations, and other genetic or environmental factors that account for the phenotypic differences.

## Acknowledgments

We are grateful to the subjects and their families for participating in this study. We thank Dr. Elena Rugarli (University of Cologne) and the UDP bioinformatics team for assistance with bioinformatics, the NINDS DNA

sequencing facility for DNA sequencing, Ms. Taryn Edsall (University of Michigan) for assistance with patient DNA sequencing, Dr. Fanny Mochel (Hôpital de La Salpêtrière) for her input in the manuscript, and Dr. Dramane Coulibaly of the Department of Neurology, Hôpital de Fann, Dakar, Sénégal for organizing the brain MRI for the Malian patient. We also thank the DNA and cell bank of UMR975 INSERM/UPMC and the SPATAX international network for providing patient DNA.

*Disclosure statement:* The authors declare no conflict of interest.

## References

- Biesecker LG, Mullikin JC, Facio FM, Turner C, Cherukuri PF, Blakesley RW, Bouffard GG, Chines PS, Cruz P, Hansen NF, Teer JK, Maskeri B, et al. 2009. The ClinSeq Project: piloting large-scale genome sequencing for research in genomic medicine. *Genome Res* 19(9):1665–1674.
- Blackstone C. 2012. Cellular pathways of hereditary spastic paraplegia. *Annu Rev Neurosci* 35:25–47.
- Blackstone C, O’Kane CJ, Reid E. 2011. Hereditary spastic paraplegias: membrane traffic and the motor pathway. *Nat Rev Neurosci* 12(1):31–42.
- Deschauer M, Gaul C, Behrmann C, Prokisch H, Zierz S, Haack TB. 2012. *C19orf12* mutations in neurodegeneration with brain iron accumulation mimicking juvenile amyotrophic lateral sclerosis. *J Neurol* 259(11):2434–2439.
- Erichsen AK, Koht J, Stray-Pedersen A, Abdelnoor M, Tallaksen CM. 2009. Prevalence of hereditary ataxia and spastic paraplegia in southeast Norway: a population-based study. *Brain* 132(Pt 6):1577–1588.
- Gonzalez MA, Acosta Lebrigo RF, Van Booven D, Ulloa RH, Powell E, Speziani F, Tekin T, Schüle R, Züchner S. 2013. GENomes Management Application (GEM.app): a new software tool for large-scale collaborative genome analysis. *Hum Mut* 34(6):842–846.
- Harding AE. 1993. Hereditary spastic paraplegias. *Semin Neurol* 13(4):333–336.
- Hartig MB, Iuso A, Haack T, Kmiec T, Jurkiewicz E, Heim K, Roeber S, Tarabin V, Dusi S, Krajewska-Walasek M, Jozwiak S, Hempel M, et al. 2011. Absence of an orphan mitochondrial protein, *c19orf12*, causes a distinct clinical subtype of neurodegeneration with brain iron accumulation. *Am J Hum Genet* 89(4):543–550.
- Hazan J, Fonknechten N, Mavel D, Paternotte C, Samson D, Artiguenave F, Davoine CS, Cruaud C, Durr A, Wincker P, Brottier P, Cattolico L, et al. 1999. Spastin, a new AAA protein, is altered in the most frequent form of autosomal dominant spastic paraplegia. *Nat Genet* 23(3):296–303.
- Hogarth P, Gregory A, Kruer MC, Sanford L, Wagoner W, Natowicz MR, Egel RT, Subramony SH, Goldman JG, Berry-Kravis E, Foulds NC, Hammans SR, et al. 2013. New NBIA subtype: genetic, clinical, pathologic, and radiographic features of MPAN. *Neurology* 80(3):268–275.
- Kruer MC, Paisan-Ruiz C, Boddaert N, Yoon MY, Hama H, Gregory A, Malandrini A, Wolter RL, Munnich A, Gobin S, Polster BJ, Palmeri S, et al. 2010. Defective *FA2H* leads to a novel form of neurodegeneration with brain iron accumulation (NBIA). *Ann Neurol* 68(5):611–618.
- Lamari F, Mochel F, Sedel F, Saudubray . 2013. Disorders of phospholipids, sphingolipids and fatty acids biosynthesis: toward a new category of inherited metabolic diseases. *J Inher Metab Dis* 36(3):411–425.
- Landouré G, Knight MA, Stanescu H, Taye AA, Shi Y, Diallo O, Johnson JO, Hernandez D, Traynor BJ, Biesecker LG, Elkahoul A, Rinaldi C, et al. 2012. A candidate gene for autoimmune myasthenia gravis. *Neurology* 79(4):342–347.
- Meilleur KG, Traoré M, Sangaré M, Britton A, Landouré G, Coulibaly S, Niaré B, Mochel F, La Pean A, Rafferty I, Watts C, Shriner D, et al. 2010. Hereditary spastic paraplegia and amyotrophy associated with a novel locus on chromosome 19. *Neurogenetics* 11(3):313–318.
- Paisan-Ruiz C, Bhatia KP, Li A, Hernandez D, Davis M, Wood NW, Hardy J, Houlden H, Singleton A, Schneider SA. 2009. Characterization of *PLA2G6* as a locus for dystonia-parkinsonism. *Ann Neurol* 65(1):19–23.
- Reid E, Rugarli EL. 2010. The online metabolic and molecular bases of inherited diseases. [http://www.ommbid.com/OMMBID/the\\_online\\_metabolic\\_and\\_molecular\\_bases\\_of\\_inherited\\_disease/b/abstract/part28/ch228.1](http://www.ommbid.com/OMMBID/the_online_metabolic_and_molecular_bases_of_inherited_disease/b/abstract/part28/ch228.1). Accessed February 20, 2011.
- Silva MC, Coutinho P, Pinheiro CD, Neves JM, Serrano P. 1997. Hereditary ataxias and spastic paraplegias: methodological aspects of a prevalence study in Portugal. *J Clin Epidemiol* 50(12):1377–1384.

# A Recurrent De Novo *FAM111A* Mutation Causes Kenny–Caffey Syndrome Type 2

Tsuyoshi Isojima,<sup>1</sup> Koichiro Doi,<sup>2</sup> Jun Mitsui,<sup>3</sup> Yoichiro Oda,<sup>4</sup> Etsuro Tokuhira,<sup>5</sup> Akihiro Yasoda,<sup>6</sup> Tohru Yorifuji,<sup>7</sup> Reiko Horikawa,<sup>8</sup> Jun Yoshimura,<sup>2</sup> Hiroyuki Ishiura,<sup>3</sup> Shinichi Morishita,<sup>2</sup> Shoji Tsuji,<sup>3</sup> and Sachiko Kitanaka<sup>1</sup>

<sup>1</sup>Department of Pediatrics, Graduate School of Medicine, The University of Tokyo, Tokyo, Japan

<sup>2</sup>Department of Computational Biology, Graduate School of Frontier Sciences, The University of Tokyo, Kashiwa, Japan

<sup>3</sup>Department of Neurology, Graduate School of Medicine, The University of Tokyo, Tokyo, Japan

<sup>4</sup>Department of Pediatrics, Ohta Nishinouchi Hospital, Koriyama, Japan

<sup>5</sup>Department of Pediatrics, Odawara City Hospital, Odawara, Japan

<sup>6</sup>Department of Medicine and Clinical Science, Kyoto University Graduate School of Medicine, Kyoto, Japan

<sup>7</sup>Department of Pediatric Endocrinology and Metabolism, Children's Medical Center, Osaka City General Hospital, Osaka, Japan

<sup>8</sup>Division of Endocrinology and Metabolism, National Center for Child Health and Development, Tokyo, Japan

## ABSTRACT

Kenny–Caffey syndrome (KCS) is a rare dysmorphic syndrome characterized by proportionate short stature, cortical thickening and medullary stenosis of tubular bones, delayed closure of anterior fontanelle, eye abnormalities, and hypoparathyroidism. The autosomal dominant form of KCS (KCS type 2 [KCS2]) is distinguished from the autosomal recessive form of KCS (KCS type 1 [KCS1]), which is caused by mutations of the tubulin-folding cofactor E (*TBCE*) gene, by the absence of mental retardation. In this study, we recruited four unrelated Japanese patients with typical sporadic KCS2, and performed exome sequencing in three patients and their parents to elucidate the molecular basis of KCS2. The possible candidate genes were explored by a de novo mutation detection method. A single gene, *FAM111A* (NM\_001142519.1), was shared among three families. An identical missense mutation, R569H, was heterozygously detected in all three patients but not in the unaffected family members. This mutation was also found in an additional unrelated patient. These findings are in accordance with those of a recent independent report by a Swiss group that KCS2 is caused by a de novo mutation of *FAM111A*, and R569H is a hot spot mutation for KCS2. Although the function of *FAM111A* is not known, this study would provide evidence that *FAM111A* is a key molecule for normal bone development, height gain, and parathyroid hormone development and/or regulation. © 2014 American Society for Bone and Mineral Research.

**KEY WORDS:** KENNY–CAFFEY SYNDROME; *FAM111A*; PARATHYROID-RELATED DISORDERS; HYPOMAGNESEMIA

## Introduction

Kenny–Caffey syndrome (KCS) (OMIM #244460, %127000) is a rare dysmorphic syndrome characterized by severe proportionate short stature with adult heights of 121 to 149 cm, cortical thickening and medullary stenosis of tubular bones, delayed closure of the anterior fontanelle, eye abnormalities, and hypocalcemia owing to hypoparathyroidism.<sup>(1–4)</sup> KCS is classified into two types according to its clinical features and inheritance pattern. Classical cases have normal intelligence and are transmitted as an autosomal dominant trait or sporadically and are called KCS type 2 (KCS2) (OMIM %127000).<sup>(5)</sup> Cases having mental and prenatal growth retardation and transmitted as an autosomal recessive trait are called KCS type 1 (KCS1) (OMIM #244460).<sup>(4,6,7)</sup>

In 2002, a study of 65 individuals from 34 pedigrees of Middle Eastern origin resulted in the identification of mutations of the tubulin-folding cofactor E (*TBCE*) gene as the cause of KCS1. *TBCE* encodes a molecular chaperone required for heterodimerization of  $\alpha$ -tubulin with  $\beta$ -tubulin.<sup>(8)</sup> KCS2 is extremely rare, with only 5 sporadic cases reported in Japan.<sup>(9–12)</sup> Because of this rarity, the cause of KCS2 has been unknown until it was recently reported to involve the “family with sequence similarity 111, member A” (*FAM111A*) gene (NM\_001142519.1) by a Swiss group in 2013.<sup>(13)</sup>

In this study, we recruited 4 Japanese patients with typical sporadic KCS2 having normal intelligence and performed whole exome sequencing in 3 unrelated trios to elucidate the molecular basis of KCS2. We hypothesized that KCS2 is caused by de novo mutations and built a de novo mutation detection pipeline to

Received in original form June 10, 2013; revised form August 21, 2013; accepted August 27, 2013. Accepted manuscript online August 31, 2013.

Address correspondence to: Sachiko Kitanaka, MD, PhD, Department of Pediatrics, Graduate School of Medicine, The University of Tokyo, 7-3-1 Hongo, Bunkyo-ku, Tokyo, 113-8655, Japan. E-mail: sachi-tyk@umin.ac.jp

Additional Supporting Information may be found in the online version of this article.

Journal of Bone and Mineral Research, Vol. 29, No. 4, April 2014, pp 992–998

DOI: 10.1002/jbmr.2091

© 2014 American Society for Bone and Mineral Research

process the raw data from exome sequencing. Using this method, we found an identical de novo mutation in *FAM111A* in all 4 patients. This and the reported independent studies provide evidence that *FAM111A* is the cause of KCS2, and R569H is a hot spot mutation for KCS2.

## Materials and Methods

### Subjects

#### Case 1

This 10-year-old girl (Fig. 1, I-1)<sup>(9)</sup> was born at 40 weeks of gestation to nonconsanguineous, healthy Japanese parents. Polysyndactyly was noticed at birth. At 3 months of age, she was referred to a pediatric endocrinologist because of growth retardation. Her body length, body weight, and head circumferences were 55 cm (−2.5 SD), 5092 g (−1.8 SD), and 37.3 cm (0.2 SD), respectively. She was found to have liver dysfunction with a serum aspartate aminotransferase (AST) level of 227 U/L (reference range 21 to 75) and serum alanine aminotransferase (ALT) level of 227 U/L (reference range 11 to 69). Basal serum insulin-like growth factor (IGF-I), calcium (Ca), and phosphorus (P) levels were within normal limits. At the age of 1 year, hypocalcemia was revealed. Her serum Ca, P, and intact parathyroid hormone (PTH) levels were 1.6 mmol/L (reference range 2.1 to 2.4), 2.6 mmol/L (reference range 0.88 to 1.4), and 11 ng/L (reference range 15 to 50), respectively, with a normal magnesium (Mg) level of 0.86 mmol/L (reference range 0.74 to 0.90). Her serum 1,25(OH)<sub>2</sub>D level, serum alkaline phosphatase level, and urine Ca/creatinine ratio were within normal ranges. Brain computed tomography (CT) revealed calcification in the basal ganglia (Fig. 2A). She was diagnosed with primary hypoparathyroidism and was treated with alfacalcidol [1 $\alpha$ (OH)D<sub>3</sub>]. At 2 years of age, she was diagnosed with KCS2 based on clinical manifestations of proportionate short stature, cortical thickening and medullary stenosis confirmed by radioscopic study (Fig. 2B), macrocephaly with delayed closure of the anterior fontanelle, eye abnormalities (hypermetropia and pseudopapilledema), and normal intelligence. Magnesium oxide was administered because of a low serum Mg level (below 0.62 mmol/L) at 3 years of age.

#### Case 2

This 16-year-old boy (Fig. 1, II-4)<sup>(10)</sup> was born at 41 weeks of gestation to nonconsanguineous, healthy Japanese parents. When he was 23 days old, he had a generalized convulsion because of hypocalcemia. At this time, his serum Ca, P, Mg, and intact PTH levels were 1.5 mmol/L, 3.1 mmol/L, 0.74 mmol/L, and undetectable, respectively. T-cell subset was normal. He was treated with alfacalcidol on the basis of a diagnosis of primary hypoparathyroidism. Magnesium sulfate was added because of his low serum Mg level at the age of 1 year. He suffered repeated bouts of acute otitis media until the age of two years. His serum IgG level was within the normal range. At 3 years and 1 month, his height, weight, and head circumference were 77.9 cm (−4.4 SD), 9.9 kg (−2.7 SD), and 47.4 cm (−1.5 SD), respectively. He had normal intelligence for his age. He was diagnosed with KCS2 based on clinical findings of proportionate short stature, medullary stenosis revealed by radiography, a widely open anterior fontanelle (Fig. 2C, skull radiograph at 9 years), and hypermetropia. He also suffered severe atopic dermatitis after

normalization of his serum Ca levels. His growth chart is shown in Fig. 2D.

#### Case 3

This 22-year-old woman (Fig. 1, III-9)<sup>(11)</sup> was born at 40 weeks of gestation to nonconsanguineous, healthy Japanese parents following an uneventful pregnancy. At 1 month, she had an episode of generalized convulsions because of hypocalcemia. At this episode, her serum Ca, P, Mg, and intact PTH levels were 1.3 mmol/L, 2.9 mmol/L, 0.49 mmol/L, and undetectable, respectively. Oral alfacalcidol administration was started on the basis of a diagnosis of primary hypoparathyroidism. At the age of 5 years 1 month, she was referred to another hospital. Her height was 84.2 cm (−5.3 SD), and her weight was 12.2 kg (−2.2 SD). She had normal intelligence. Brain CT revealed fine calcification in the basal ganglia. Based on clinical manifestations of proportionate short stature, medullary stenosis of the long bones typical of KCS, a 1 × 1-cm opening of her anterior fontanelle, normal intelligence, and hypermetropia, she was diagnosed with KCS2. The patient was started with a combination therapy of vitamin D and magnesium sulphate. Fig. 2E shows her radiograph at 14 years of age.

#### Case 4

This 38-year-old man (Fig. 1, IV-13)<sup>(12)</sup> was born at 40 weeks of gestation to nonconsanguineous, healthy Japanese parents following an uneventful pregnancy. At 8 days of age, he had a generalized convulsion, and hypocalcemia (0.75 mmol/L) and hypomagnesemia (0.18 mmol/L) were detected. The convulsion was controlled by intravenous administration of Ca gluconate and magnesium sulfate until he was 15 days old. At 4 years of age, he again had an episode of generalized convulsion because of hypocalcemia. At this episode, his serum Ca, P, and intact PTH levels were 1.2 mmol/L, 2.6 mmol/L, and undetectable, respectively. He was diagnosed with primary hypoparathyroidism, and oral alfacalcidol and Ca lactate administration were started. He suffered repeated acute otitis media during infancy and was affected with empyema and bacterial meningitis at 4 years of age. Hypogammaglobulinemia was found, and he was administered gamma globulin intermittently. At 12 years of age, he was referred to another hospital for further investigation. His height was 99 cm (−6.3 SD), and his weight was 16.2 kg (−3.3 SD). He had normal intelligence with an intelligence quotient score of 105. Brain CT revealed fine calcification in the basal ganglia. Based on clinical manifestations of proportionate short stature, medullary stenosis of the long bones, a 4.2 × 1.8-cm opening of his anterior fontanelle, and eye abnormalities (hypermetropia, amblyopia, and pseudopapilledema), he was diagnosed with KCS2. Mg loading and Ca restriction tests revealed that his hypoparathyroidism was secondary to hypomagnesemia. The patient was then changed from vitamin D and Ca lactate to magnesium sulfate treatment, which successfully corrected his serum Ca levels.

We recruited these 4 Japanese patients with clinically diagnosed typical sporadic KCS2 (Fig. 1). Supplemental Table S1 (TBL S1) summarizes the clinical characteristics of the 4 patients. We obtained peripheral blood samples from all 4 patients, together with those of 9 unaffected parents or siblings, with informed consent for DNA analysis (Fig. 1). The study was performed with the approval of the Ethics Committee of The University of Tokyo and of each institution where the samples



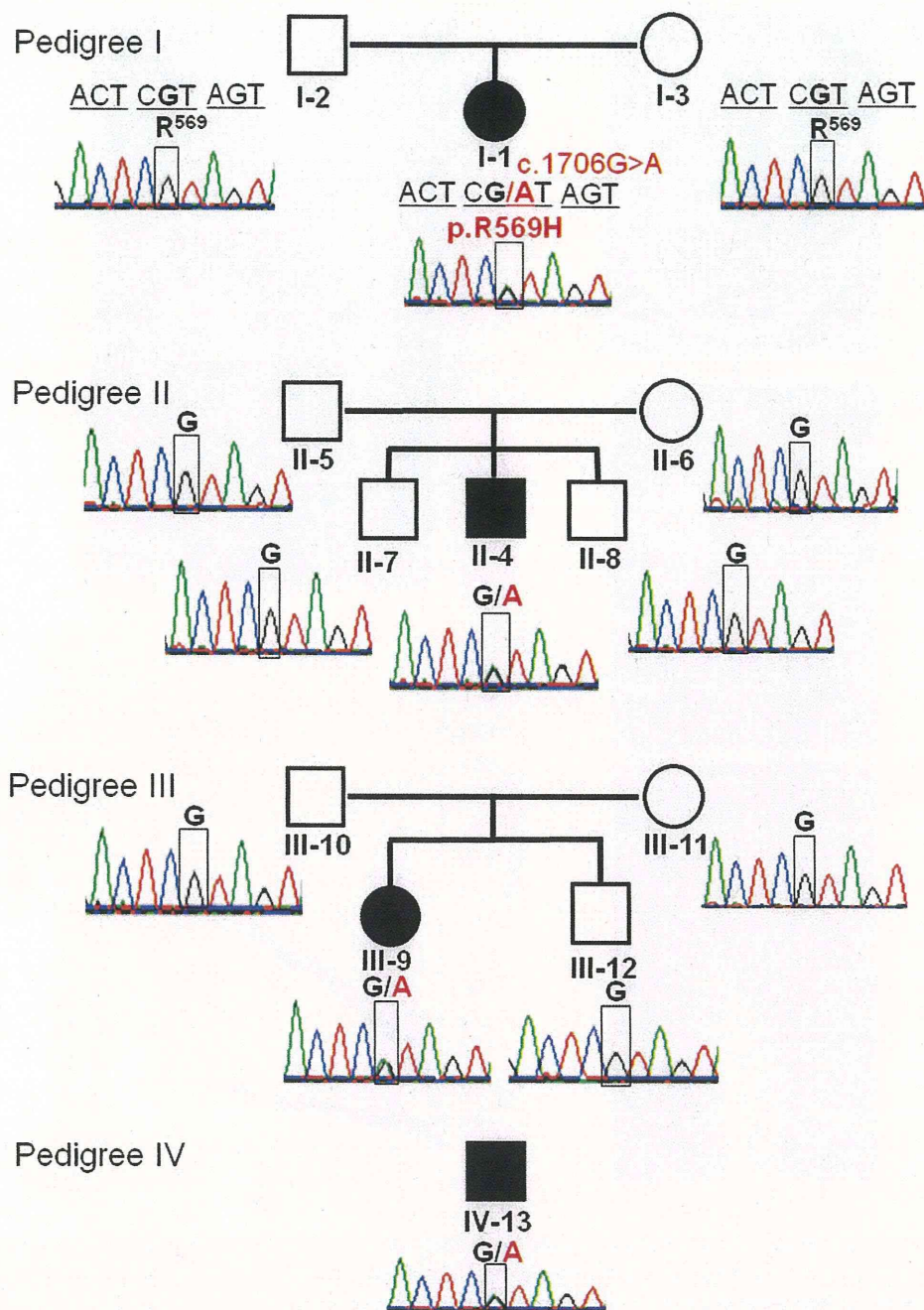


**Fig. 1.** Four pedigrees analyzed in this study, showing the chromatograms of Sanger sequencing reactions of the *FAM111A* mutation in patients and family members. Data were obtained by Sanger sequencing during the confirmation process. All mutations were checked by bidirectional sequencing. In each pedigree, a black symbol represents the proband, a square indicates a male, and a circle shows a female. In the chromatogram, black letters indicate the wild-type nucleotide sequence. Nucleotides in red indicate mutations. R569H was identified in all probands but not in any of the unaffected family members.

were collected, and conducted in accordance with the Declaration of Helsinki. Genomic DNA was extracted from peripheral white blood cells of the patients and family members using a QIAamp DNA Blood Midi Kit (Qiagen, Hilden, Germany). Healthy Japanese volunteers were recruited, and DNA was extracted with informed consent.

#### Exome sequencing

Exome sequences were enriched using a TruSeq Exome Enrichment Kit (Illumina, San Diego, CA, USA) from 1  $\mu$ g of genomic DNA, according to the manufacturer's instructions. The captured DNA samples were subjected to massively parallel

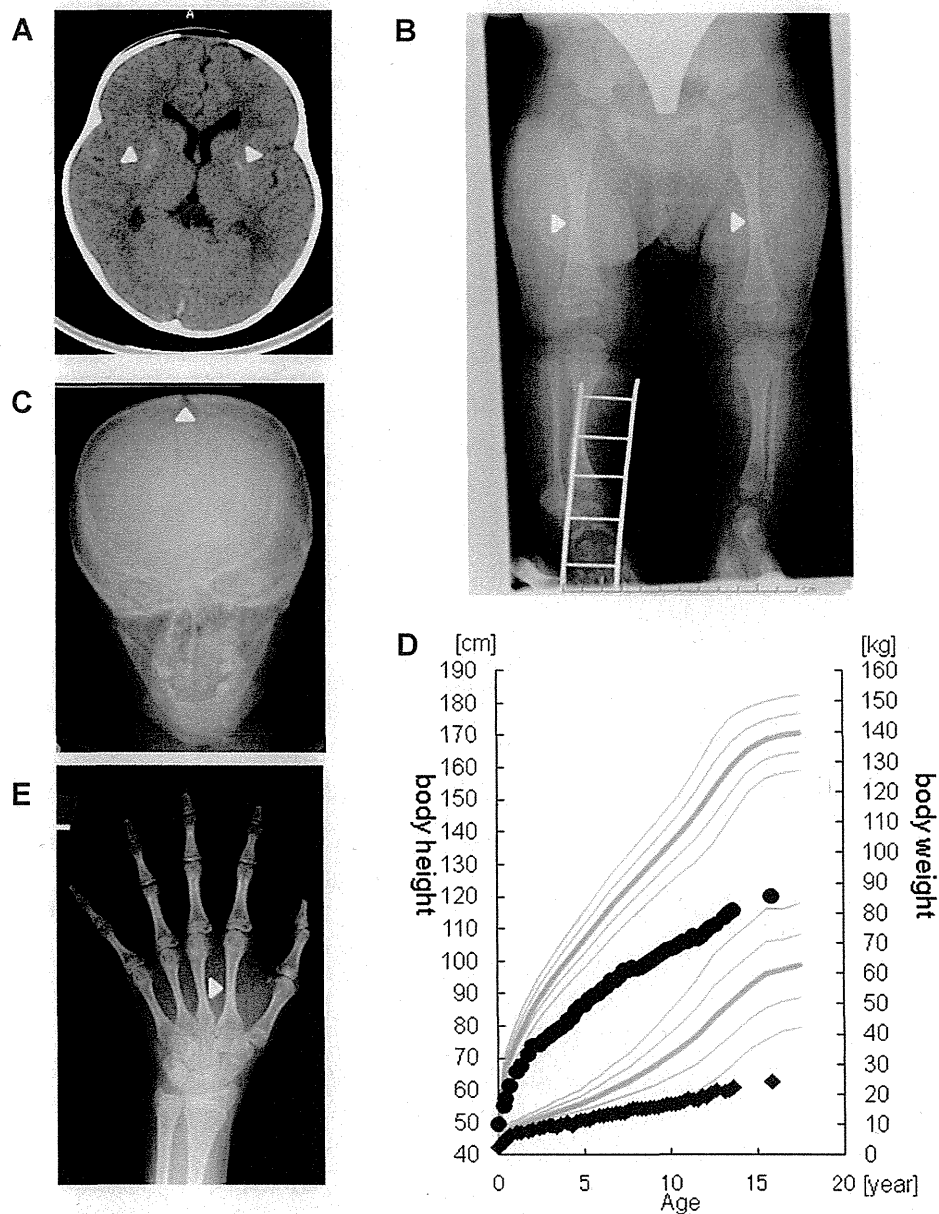


**Fig. 2.** Radiographic studies and growth charts of probands. (A) Brain computed tomography of patient I-1. The arrowheads indicate calcification in the basal ganglia. (B) Radiograph of patient I-1 at diagnosis. Cortical thickening and medullary stenosis are evident. The object shown in the right leg is used for fixing a peripheral catheter. (C) Radiograph of patient II-4 at age 9 years. It is of note that the anterior fontanelle is open. (D) Growth chart of patient II-4 superimposed on the standard growth chart for a Japanese boy. Black circles indicate the patient's height, and black squares indicate his weight. (E) Radiograph of patient III-9. Cortical thickening and medullary stenosis can be observed.

sequencing (100-bp paired-end reads) on an Illumina HiSeq2000 sequencing system (Illumina). An average of 95 million reads of the sequence data was obtained for each individual. On an average, 98.50% of the total bases were mapped to the reference genome with a mean coverage of  $140.5 \times$ , which encompassed 91.94% of the targeted regions with coverage  $>10 \times$  (Supplemental Table S2). The Burrows-Wheeler Aligner (BWA) package<sup>(14)</sup> and SAMtools<sup>(15)</sup> were used as default settings for alignment of raw reads and detection of single-nucleotide variants (SNVs) and indels. Subsequently, SNVs and indels were

filtered with three trio samples (ie, pedigrees I, II, and III) (Supplemental Fig. S1). We extracted both homo/heterozygous nonsynonymous coding variants, which were called in the proband, and filtered these candidates using the following three steps:

Step 1: Using candidate de novo mutations that are homozygous references in both parents and are supported by 10 or more high-quality reads at the mutated sites for every trio member.

Step 2: Using reliable homozygous references in each parent such that the likelihood of heterozygosis,  $nC_i(1/2)^i(1/2)^{n-i}$ , is less than that of homozygosis,  $nC_i(999/1000)^i(1/1000)^{n-i}$ , where the average error rate is assumed to be 1/1000,  $n$  represents the number of total reads, and  $i$  is the number of reads consistent with the reference. One may have an impression that this condition does not often hold true; however, we often observed cases that violated this condition, especially when the reference base was mutated into one of the other three bases with an almost equal probability.

Step 3: Using reliable de novo mutations of the proband such that the number of alternative allele reads was at least 30% among the total reads, which is the condition proposed in a recent report.<sup>(16)</sup>

### Sanger sequencing

Sanger sequencing was performed to detect *TBCE* (*KCS1*) and validate the presence of each variant detected by exome sequencing in patients with *KCS2* and the absence of each in the genomes of the parents and siblings. The entire coding region and exon–intron boundaries of *TBCE* and *FAM111A* were amplified from genomic DNA by polymerase chain reaction (PCR) using the designed PCR primers (Supplemental Table S3). [TBL S3] Subsequently, PCR products were sequenced using an ABI Prism BigDye Terminator Cycle Sequencing Ready Reaction Kit (PE Applied Biosystems, Foster City, CA, USA) and the forward and reverse primers used for PCR amplification. Direct sequencing in both directions was performed on an autosequencer (PE Applied Biosystems 3130 × 1, Genetic Analyzer).

### *FAM111A* mRNA expression analysis

Total RNA was prepared using ISOGEN reagent (Nippon Gene, Osaka, Japan), according to the manufacturer's instructions, from peripheral white blood cells of the patients and family members. Total RNA (4 μg) was used to synthesize cDNA with the SuperScript Preamplification System for first-strand cDNA synthesis (Life Technologies, Rockville, MD, USA). mRNA levels were measured using an ECO real-time PCR system (Illumina) and KAPA SYBR Fast qPCR Kit (Kapa Biosystems, Woburn, MA, USA) using the following primer pairs: *FAM111Ae5-2F* and *FAM111Ae5-2R*; *FAM111Ae5-3F* and 5'-CCTCATCACTCATCTTC-TACATCC-3'; *GAPDH*, 5'-GAAGGTGAAGTCCGGAGTC-3' (F) and 5'-GAAGATGGTGATGGGATTC-3' (R). The relative mRNA level was calculated using an arithmetic formula based on the difference between the threshold cycle of a given target cDNA and that of an endogenous reference cDNA. Direct sequencing of the RT-PCR products was performed by Sanger sequencing as for DNA samples.

## Results

We first confirmed by Sanger sequencing that none of the 4 patients had *TBCE* mutations. This finding, together with the fact that all the patients were of normal intelligence, distinguishes these patients from patients with *KCS1*.

We hypothesized that these sporadic cases may be caused by de novo mutations in novel nonsynonymous coding variants. Whole exome sequencing was performed for 3 patients (I-1, II-4, and III-9; Fig. 1) and their parents (I-2, I-3, II-5, II-6, III-10, and III-11; Fig. 1). Statistical data of exome sequencing experiments are

shown in Supplemental Table S2. The candidate variants were selected according to the processes described in Materials and Methods based on the de novo mutation detection pipeline designed in the present study (Supplemental Fig. S1). Supplemental Table S4 [TBL S4] summarizes the results of filtering to detect candidate genes for *KCS2*. To select variants as candidate mutations for *KCS2*, variations that caused amino acid substitution were extracted, which resulted in 11,024 (pedigree I), 10,828 (pedigree II), and 11,020 (pedigree III) SNVs and indels. After three filtering steps, 5 (pedigree I), 5 (pedigree II), and 6 (pedigree III) SNVs were identified. Among the candidate genes filtered using the three aforementioned filtering steps, only one single gene, *FAM111A* (NM\_001142519.1), was shared among all 3 families. Sanger sequence analysis of all exons of *FAM111A* confirmed an identical c.1706G > A heterozygous mutation in exon 5 in all 3 patients (Fig. 1). This mutation is predicted to result in substitution of arginine to histidine in codon 569 (R569H). None of the unaffected family members had this mutation, indicating that R569H was a de novo mutation. This mutation was also found in an additional unrelated patient (IV-13).

R569H is not present in 373 Japanese healthy control subjects of an in-house exome database, and not in another 100 alleles from 50 unrelated healthy Japanese individuals by Sanger sequencing. It was also not found in the Japanese SNP control database established by the National Bioscience Data Base Center that has 1 million genome-wide SNPs of 700 samples ([http://gwas.biosciencedbc.jp/snpdb/snp\\_top.php](http://gwas.biosciencedbc.jp/snpdb/snp_top.php)), nor among 6500 samples listed on the exome variant server (<http://evs.gs.washington.edu/EVS/>), implying that the minor allele frequency is less than 0.01% in these data. However, one SNP was found in the 1000 Genomes database at R569 (rs184251651), which results in substitution to "cysteine" (minor allele frequency 0.1%).

We assessed the functionality of the R569H mutation using the Sorting Intolerant From Tolerant (SIFT) (<http://sift.jcvi.org>) and Polymorphism Phenotyping 2 (PolyPhen2) (<http://genetics.bwh.harvard.edu/pph2>) tools, by homology modeling and threading. These *in silico* studies predicted R569H as "tolerated" and "benign," respectively.

We analyzed the expression levels of *FAM111A* mRNA in peripheral white blood cells by real-time PCR. *FAM111A* expression levels in the patients were comparable with those in unaffected family members and normal controls (data not shown). We also found that mutant and wild-type *FAM111A* were equivalently expressed in the patients, which were identified by sequencing the reverse-transcribed PCR products.

## Discussion

In the present study, we identified *FAM111A* as the gene responsible for *KCS2* by applying an exome sequencing strategy, and we identified a heterozygous identical de novo *FAM111A* mutation, R569H, in 4 Japanese patients with *KCS2*. While preparing this article, another independent research group from Switzerland reported similar findings following whole exome sequencing of the patients.<sup>(13)</sup> They reported that all 5 clinically diagnosed *KCS2* patients had de novo *FAM111A* mutations. Most interestingly, 4 of the 5 patients from different countries had the same R569H mutation as detected in our patients. Our 4 pedigrees are unrelated to each other and live in different areas in Japan. Moreover, the parents of the 3 patients did not have the mutation, suggesting that this recurrent mutation was caused by sporadic mutation. Taken together, these two independent

studies confirm that *FAM111A* is the causative gene for KCS2, and R569H is the hot spot mutation of KCS2.

*FAM111A* encodes a previously uncharacterized protein consisting of 611 amino acids. The carboxy-terminal half of the protein has homology to trypsin-like peptidases, and the catalytic triad specific to such peptidases is conserved.<sup>(17)</sup> Transcriptional expression of *FAM111A* is ubiquitous according to the human protein atlas (<http://www.proteinatlas.org/ENSG00000166801/normal>). It is expressed in the parathyroid gland and bone, but the expression levels are similar to those in other tissues. *FAM111A* has 35% amino acid homology to *FAM111B*, a paralog located on 11q12.1 at a distance of only 16 kb from *FAM111A*. The functions of *FAM111A* and *FAM111B* are largely unknown. A recent report showed that *FAM111A* functions as a host range restriction factor and is required for viral replication and gene expression by specifically interacting with Simian Virus 40 large T antigen (LT).<sup>(17)</sup> In addition, *FAM111A* mRNA and protein levels have been shown to be regulated in a cell cycle-dependent manner with the lowest expression during the G0 or quiescent phase and peak expression during the G2/M phase.<sup>(17)</sup> Another recent report revealed that variants in the region including *FAM111A* and *FAM111B* were associated with prostate cancer.<sup>(18)</sup> However, the clinical course of disease in our 4 patients revealed neither increased viral infections nor carcinogenesis up to early adulthood.

In silico analyses suggested that the de novo mutation (R569H) would not significantly affect the function of *FAM111A*. We also found that the mutant *FAM111A* mRNA was expressed similarly to the wild type in peripheral blood cells. This raises the question of how this mutation causes KCS2. One hypothesis is that this mutation does not cause loss of function of the protein but rather modulates its peptidase activity for a particular target peptide in a mutant-specific way. Another possibility is that *FAM111A* functions with some physiological partner(s) and the disease occurs as a result of specific modulation of this putative network. This may fit the observation that *FAM111A* is regulated in a cell-dependent manner and interacts with the LT C-terminal region.<sup>(17)</sup> We speculate that one of the candidate partner proteins is TBCE because KCS1 and KCS2 share distinctive phenotypic features: skeletal dysmorphic features and primary hypoparathyroidism.

Some diseases are caused by specific mutations of a single gene. Some mutations may cause a gain-of-function effect, as in achondroplasia or McCune–Albright syndrome,<sup>(19,20)</sup> whereas others have an unknown function, as in Caffey syndrome caused by mutations in *COL1A1*<sup>(21)</sup> or in several diseases related to *FGFR3*. In this study, we found that a specific mutation (R569H) of *FAM111A* would lead to KCS2. Intriguingly, one SNP was found in the 1000 Genomes database at R569 (rs184251651), which results in substitution to “cysteine.” This SNP has been reported to have minor allele frequency of 0.1% (only one allele) and is not validated. Moreover, the absence of the SNP in 6500 samples in the exome variant server suggests a possibility of sequencing error in the database. Nevertheless, it might be speculated that a specific change to “histidine” may lead to an unidentified function of this protein resulting in KCS2, which is not caused by other amino acids. This hypothesis will be supported by the fact that this amino acid is not well conserved among various species (Fig. 3).

It is reported that 95% and 97% of KCS1 cases had prenatal and postnatal growth retardation, and mental retardation, respectively.<sup>(22)</sup> In contrast, most of the reported KCS2 patients, including our patients with *FAM111A* mutations, had normal

	R569H
<i>Homo sapiens</i>	GFAYTYQNETR <b>S</b> SIIEFGSTME
<i>Macaca mulatta</i>	GFAYTYQNQTR <b>S</b> SIIEFGSTME
<i>Ornithorhynchus anatinus</i>	GYLHTYRRRV <b>R</b> GIIEIGYSMD
<i>Equus caballus</i>	GFPYLYPNTV <b>E</b> TIIEFGFTLE
<i>Oryctolagus cuniculus</i>	GFAYEYQHEI <b>S</b> SIIEFGSAMK
<i>Loxodonta africana</i>	GYFYKYQNGF <b>S</b> SIIEFGSAMK
<i>Cricetulus griseus</i>	GYTCEYQSGV <b>S</b> NIIEFGSTME
<i>Rattus norvegicus</i>	GITCTDQNGV <b>E</b> NIIEFGFTME
<i>Mus musculus</i>	GITCTYQAGV <b>S</b> NIIEFGSIME
<i>Cavia porcellus</i>	GCTEKYGG <b>T</b> FHIIIEFGSAMQ
<i>Anolis carolinensis</i>	GYLYRGRCKE <b>K</b> SIIIEFGYSMM

**Fig. 3.** Homologous comparison of the altered protein. Letters in the rectangular box indicate the human *FAM111A* R569 residue. It is of note that R569 is not well conserved among various species.

birth weight and length and normal intelligence (Supplemental Table S1).<sup>(13)</sup> These phenotypic differences between KCS1 and KCS2 suggest that the *FAM111A* mutation does not affect bone development and height gain in the fetus but becomes important postnatally. It also suggests that the *FAM111A* mutation does not affect mental development. Now that *FAM111A* has been identified as a causative gene for KCS2, further studies on the physiological function of *FAM111A* and TBCE should be performed to uncover the phenotypic differences between these two types.

There are several human diseases, as well as mouse models of hypoparathyroidism, caused by aberrations in the cascade of genes indispensable for the development and regulation of the parathyroid gland.<sup>(23,24)</sup> To date, *FAM111A* is not known to relate to any of these genes. There have been only a few reports describing the pathophysiology of hypoparathyroidism in KCS. Absence of the parathyroid glands has been reported in some patients with KCS2 and KCS1.<sup>(25,26)</sup> In contrast, some patients do not have hypoparathyroidism from early infancy, suggesting the presence of some parathyroid gland as in our patient I-1.<sup>(4,27)</sup> Furthermore, hypoparathyroidism may be secondary to hypomagnesemia as in our patient IV-13. Considering the fact that all of our 4 patients as well as another reported KCS2 case had hypomagnesemia,<sup>(4)</sup> *FAM111A* might be involved in magnesium homeostasis. Although further investigation is necessary to reveal the cause of hypoparathyroidism in KCS2, this study shows that a new gene, *FAM111A*, is indispensable for PTH development and/or regulation.

In conclusion, our finding that all 4 Japanese KCS2 patients we tested have the same de novo mutation (R569H) of *FAM111A* indicates that KCS2 is caused by a heterozygous mutation of *FAM111A*, and R569H is the hot spot mutation in patients with KCS2. Although the function of *FAM111A* is largely unknown, this study provides evidence that *FAM111A* is a key molecule for normal bone development, height gain, and PTH development and/or regulation. Our finding further creates a new research area in the fields associated with shared phenotypic features in KCS and different phenotypes between KCS1 and KCS2.

## Disclosures

TI has received research grants and speaker's fees from Novo Nordisk and has received speaker's fees from Eli Lilly. SK has received research grants and speaker's fees from Novo Nordisk,